



INTERNATIONAL JOURNAL OF DEVELOPMENT MATHEMATICS

ISSN: 3026-8656 (Print) | 3026-8699 (Online)

journal homepage: <https://ijdm.org.ng/index.php/Journals>



A Simulation-Based Analysis of Model for Coronavirus Disease Using Nonstandard Finite Difference Scheme

Shah Zeb^{a*}, Noreen Kausar^b, Muhammad Rafiq^c, Muhammad Irfan^d, Ihsan U. Khan^d and Muhammad Bilal^e

^a*School of Distance Education, Universiti Sains Malaysia, 11800, Penang, Malaysia.*

^b*Department of Mathematics, University of Management and Technology, CII Johar Town, Lahore, 54770, Punjab, Pakistan.*

^c*Department of Mathematics, Namal University, 30KM Talagang Road, Mianwali, 42250, Pakistan.*

^d*Department of Mathematics, Institute of Numerical Sciences, Gomal University, Dera Ismail Khan 29050, KPK, Pakistan.*

^e*Department of Mathematics, University of Layyah, Layyah, 31200, Pakistan.*

ARTICLE INFO

Article history:

Received 10 September 2025

Received in revised form 20 November 2025

Accepted 30 November 2025

Keywords:

COVID-19 mathematical model; NSFD scheme; Local and global stability, Numerical simulations

MSC 2020 Subject classification: 34A34, 92D30, 34K20, 92D25.

ABSTRACT

Infectious diseases such as MERS, SARS, AIDS, COVID-19, and polio have completely decimated the social and economic structure of the global population. The COVID-19 is an infectious disease that spreads rapidly all around the world. In the present article, the novel COVID-19 mathematical model containing the resistive class together with the class of quarantine is offered and examined. The analysis of disease-free and endemic equilibria stability focuses on the basic reproductive number, which is examined in detail. The non-standard finite difference (NSFD) scheme is established which conserves important characteristics of the continuous model and provides precise results for all finite step sizes. It is shown that NSFD is unconditionally convergent, solutions remain positive and produces better outcomes in all respect. To demonstrate the local and global stability of the equilibria for the NSFD scheme, multiple existing criteria from the literature are used. To sustenance the theoretical discoveries and illustrate the compensations of NSFD scheme, numerical simulations are also conducted. Numerical simulations indicate that NSFD scheme maintains the key aspects of the continuous model. The data which is provided in this paper can be utilized to monitor the spread of the transmissible COVID-19 disease.

1. Introduction

On December 31, 2019, the coronavirus disease 2019 (COVID-19) persisted in Wuhan City, Hubei Province, China. It quickly then spread all over the world and an epidemic initiated. due to an abrupt spike in the intensity of transmission, the World Health Organization (WHO) considered the COVID-19 outbreak to be a global pandemic on March 11. Direct interaction and aerosolized droplets may pass the infectious disease COVID-19 from one person to another. The WHO has also enforced security measures, such as isolation, quarantine, heightened home confinement, endorsement of face mask use, travel restrictions, closure of public places, and cancellation of events. Around 517 million confirmed cases and over 6.25 million fatalities were recorded worldwide by Aba Oud *et al.* (2022); Mahmoudi *et al.* (2021); Sardar *et al.* (2020); Duan *et al.* (2020) & Klompas (2022).

Mathematical modeling is a useful tool for investigating real world spectacles and procedures of Ogana, W *et al.* (2021); Ivorra *et al.* (2020); Aljohani *et al.* (2024); Khan *et al.* (2023); Medvedeva *et al.* (2024); Shokri *et al.* (2022);

*Corresponding author. Tel.: +923020706394

E-mail address: shahzeb@student.usm.my (Shah Zeb)

<https://doi.org/10.62054/ijdm/0204.02>

Simos *et al.* (2024) & Medvedeva *et al.* (2024). The purpose of epidemic disease mathematical models is to investigate the nonlinear mechanism involved in the behaviours of infectious diseases and to develop the most effective suitable method for controlling them. It is usually acknowledged that mathematical models can be employed to forecast the occurrence of infectious diseases. This allows predicting the possible outcomes of an epidemic disease, which is beneficial for public health initiatives. Compartmental models can be used as a fundamental mathematical framework to investigate the intricate dynamics of epidemiological procedures given by Rao, F *et al.* (2019). Many researchers initially endeavor to comprehend the dynamics of a disease by using mathematical models, and then they create prevention and treatment strategies by Brauer *et al.* (2017); Castillo-Chave *et al.* (2002) & Kumar *et al.* (2019). Mathematical model is also a useful tool for demonstrating COVID-19 dispersion, and assumptions may be made using its simulations. During the COVID-19 outbreak, modeling caught the attention of numerous biologists, mathematicians, pharmacists, and epidemiologists. During COVID-19 epidemic, the WHO top objective was to evaluate the efficacy and safety of vaccines. To ensure vaccination efficacy, WHO works collaboratively with researchers from all around the world to develop and put into practice international standards and norms. A number of publications of Acuna-Zegarra, M.A *et al.* (2020); Francis *et al.* (2022), Kaur *et al.* (2020) & Zeb, S. *et al.* (2024) are recently available on the effectiveness of vaccines that have been introduced. The mathematical modeling is a valuable means in this regard to focus on the process of how an unstoppable infection can spread over a community.

There are various mathematical models of Ahmad, S *et al.* (2021); Ali *et al.* (2021); Moore *et al.* (2021); Contreras *et al.* (2021) & Adak *et al.* (2021) that are accessible in the literature that do not take the quarantine into account, despite the fact that it is essential to the control of the COVID-19 disease. Recently in Ahmad, S *et al.* (2021), the authors take into account the COVID-19 mathematical model together with resistive compartment in addition to the quarantine class. The model is distinct from earlier models observed in the literature due to the occurrence of resistive and quarantine classes together. The authors examined the necessary analytical results, containing the stability of equilibria for the continuous model. The intention of present paper is to control the transmission of COVID-19 and examine its extortions to the health of public. The NSFD scheme is created to evaluate different characteristics of the model and show their ecological viability and suitability. The results of this study show that the previously mentioned scheme adequately defines the continuous model for any step size and is dynamically consistent. The novelty lies in applying a fuzzy NSFD scheme to COVID-19 modeling with dynamic fuzzy parameters, offering improved stability and realism compared to existing deterministic or crisp NSFD approaches of Diekmann *et al.* (2010).

The paper is managed in the manner listed below. The mathematical model is given in Section 2, and each parameter is described thoroughly. In Section 3, the disease-free and endemic equilibria of the model are deliberated. The reproductive number, which is the best substantial threshold quantity worked to explain the local and global stability of equilibria is presented in Section 4. In section 5, the advanced discrete NSFD is constructed for the given model. In the same section, the local and global stability of both the equilibria for NSFD scheme are investigated using a variety of existing criteria. The numerical simulations are also presented at each section to validate the theoretical conclusions. The conclusions are offered is last section.

2. Methodology

2.1 Mathematical model

The dynamical system of COVID-19 given by Ahmad, S et al. (2021) based on susceptible population S , resistant population H , infected population I and quarantine population Q , respectively is given as follows. If the total population be denoted by $N(t)$, then $N(t) = Q(t) + I(t) + H(t) + S(t)$. Fig.1 shows a thorough explanation of the model.

$$\begin{aligned} \frac{dS(t)}{dt} &= \Lambda - \gamma_1 S(t)I(t) - (\omega + \mu)S(t) \\ \frac{dH(t)}{dt} &= \epsilon - \tau H(t)I(t) + \Psi I(t) - (\omega + \mu)H(t) \\ \frac{dI(t)}{dt} &= \gamma_1 S(t)I(t) + \tau H(t)I(t) + \sigma Q(t) - (\omega + \mu + \eta + \Psi)I(t) \\ \frac{dQ(t)}{dt} &= \eta I(t) - (\omega + \mu + \sigma)Q(t). \end{aligned} \tag{1}$$

The parameters and their detailed depiction are presented in Tab. 1. All of the parameters are taken to be constant positive constants.

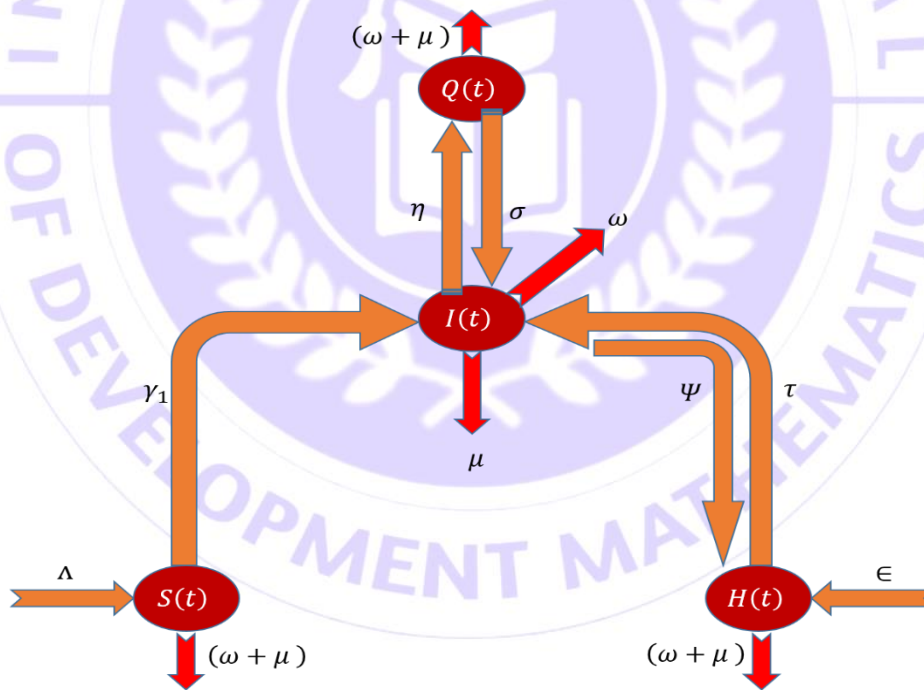


Figure 1. The flow chart of COVID-19

Table1: Parameters and their biological meanings.

Parameters	Depiction of parameters	Reference
Λ	Rate of susceptible recruitment	Assumed
γ_1	Rate of disease spread. Captures how quickly an infectious person generates new infections per unit time	Assumed
ω	Rate of natural fatality	Assumed
τ	Rate of transmission of disease in well human. Represents transmission from infectious to apparently well/active community members	Assumed
μ	Decease rate of individuals due to disease related virus	Assumed
ϵ	Rate of healthy human recruitment	Assumed
Ψ	Rate at which people are cured in quarantine class. Represents recovery (or successful treatment) rate for quarantined/isolated individuals	Assumed
σ	Rate at which people are infected in quarantine class. Captures residual transmission occurring inside quarantine	Assumed
η	Rate at which infected people are transferred into quarantine class. Describes the speed of case detection and movement of infectious individuals into quarantine/isolation	Assumed

2.2 Equilibria of model

All classes other than susceptible and resistant classes are set to zero in order to govern the disease-free equilibrium (DFE) point, i.e. if $Q, I = 0$, then we obtain $S = \frac{\Lambda}{\omega + \mu}$, $H = \frac{\epsilon}{\omega + \mu}$. Consequently, the DFE point denoted by $E^0(S^0, H^0, I^0, Q^0)$ becomes $E^0 = \left(\frac{\Lambda}{\omega + \mu}, \frac{\epsilon}{\omega + \mu}, 0, 0\right)$.

We solve the system (1) simultaneously for S, H, I and Q to get the endemic equilibrium (EE) point. If the EE point be denoted by $E^*(S^*, H^*, I^*, Q^*)$, then from the model (1), we get $S^*(t) =$

$$\frac{\Lambda}{\gamma_1 I^*(t) + (\omega + \mu)}, H^*(t) = \frac{\epsilon + \Psi I^*(t)}{\tau I^*(t) + (\omega + \mu)}, I^*(t) = \frac{\sigma Q^*(t)}{(\omega + \mu + \eta + \Psi) - \gamma_1 S^*(t) S^*(t) - \tau H^*(t)} \text{ and } Q^*(t) = \frac{\eta I^*(t)}{(\omega + \mu + \sigma)}.$$

2.3 Reproduction number (R_0)

The quantity R_0 by Akinpelu *et al.* (2018) is a significant threshold that determines whether or not a transmissible disease will propagate among people. To obtain R_0 , we use transmission $F(x)$ and translation $\mathcal{V}(x)$ matrices, respectively. The matrices mentioned above can be represented for model (1) as

$$F(x) = \begin{bmatrix} \gamma_1 S^0 + \tau H^0 & 0 \\ 0 & 0 \end{bmatrix} \text{ and } \mathcal{V}(x) = \begin{bmatrix} \omega + \mu + \eta + \Psi & -\sigma \\ -\eta & \omega + \mu + \sigma \end{bmatrix}.$$

From above, we get

$$F = \begin{bmatrix} \frac{\gamma_1 \Lambda + \epsilon \tau}{(\omega + \mu)} & 0 \\ 0 & 0 \end{bmatrix} \text{ and } \mathcal{V} = \begin{bmatrix} \omega + \mu + \eta + \Psi & -\sigma \\ -\eta & \omega + \mu + \sigma \end{bmatrix}.$$

As we know that

$$R_0 = \rho(F\mathcal{V}^{-1}).$$

Therefore, using F and \mathcal{V} we obtain

$$R_0 = \frac{(\gamma_1 \Lambda + \epsilon \tau)(\omega + \mu + \sigma)}{(\omega + \mu)[(\omega + \mu + \eta + \Psi)(\omega + \mu + \sigma) - \sigma \eta]}.$$

2.4 The non-standard finite differences (NSFD) scheme

The most important purpose of this section is to construct discrete NSFD scheme that is dynamically compatible with the continuous model (1). The NSFD schemes are widely used in ecology, epidemiology, and population modeling's Darti *et al.* (2020); Ochoche *et al.* (2014); Rao *et al.* (2018); Shabbir *et al.* (2019), Dang *et al.* (2019) & Zeb, S. *et al.* (2026). To produce NSFD scheme for model (1), we employ S_n, H_n, A_n and Q_n as mathematical measures of $S(t), H(t), I(t)$ and $Q(t)$ at $t = n\varphi$ where $n = 0, 1, 2, \dots$ and φ indicates step size. By employing the Mickens concept Mickens (1994), we can develop the NSFD scheme for system (1) as given below.

$$\begin{aligned} \frac{S_{n+1} - S_n}{\varphi} &= \Lambda - \gamma_1 S_{n+1}(t) I_n(t) - (\omega + \mu) S_{n+1}(t) \\ \frac{H_{n+1} - H_n}{\varphi} &= \epsilon - \tau H_{n+1}(t) I_n(t) + \Psi I_n - (\omega + \mu) H_{n+1}(t) \\ \frac{I_{n+1} - I_n}{\varphi} &= \gamma_1 S_n(t) I_{n+1}(t) + \tau H_n(t) I_{n+1}(t) + \sigma Q_n - (\omega + \mu + \eta + \Psi) I_{n+1}(t) \\ \frac{Q_{n+1} - Q_n}{\varphi} &= \eta I_n(t) - (\omega + \mu + \sigma) Q_{n+1}(t). \end{aligned} \quad (2)$$

The NSFD scheme (2) can be reorganized to get an explicit form as

$$\begin{aligned} S_{n+1} &= \frac{S_n + \varphi \Lambda}{(1 + \varphi(\gamma_1 I_n + (\omega + \mu)))} \\ H_{n+1} &= \frac{H_n + \varphi(\epsilon + \Psi I_n(t))}{(1 + \varphi(\tau I_n + (\omega + \mu)))} \\ I_{n+1} &= \frac{I_n + \varphi \sigma Q_n(t)}{(1 + \varphi((\omega + \mu + \eta + \Psi) - \gamma_1 S_n - \tau H_n))} \\ Q_{n+1} &= \frac{Q_n + \varphi \eta I_n}{(1 + \varphi(\omega + \mu + \sigma))}. \end{aligned} \quad (3)$$

To describe the local asymptotic stability (LAS) of DFE and EE points, we suppose that

$$\left. \begin{aligned} P_1 = S_{n+1} &= \frac{S + \varphi \Lambda}{(1 + \varphi(\gamma_1 I + (\omega + \mu)))} \\ P_2 = H_{n+1} &= \frac{H + \varphi(\Psi I + \epsilon)}{(1 + \varphi(\tau I + (\omega + \mu)))} \\ P_3 = I_{n+1} &= \frac{I + \varphi \sigma Q}{(1 + \varphi((\omega + \mu + \eta + \Psi) - \gamma_1 S - \tau H))} \\ P_4 = Q_{n+1} &= \frac{Q + \varphi \eta I}{1 + \varphi(\omega + \mu + \sigma)} \end{aligned} \right\} \quad (4)$$

3. Local stability of equilibria

The Schur-Cohn criterion of Brauert *et al.* (2001) & J.Jia *et al.* (2011), which is stated in the subsequent Lemma 1, will be used to demonstrate LAS of DFE point.

Lemma 1 The roots of $\lambda^2 - B\lambda + C = 0$ assurance $|\lambda_k| < 1$ for $k = 1, 2$, if and only if the subsequent requirements are satisfied.

1. $C < 1$,
2. $1 + B + C > 0$,
3. $1 - B + C > 0$,

where B stands for trace and C for Jacobian matrix determinant.

Theorem:1 The DFE point E^0 of the NSFD scheme (3) is LAS for all $\varphi > 0$ whenever $R_0 < 1$.

Proof Consider the Jacobian matrix

$$J = \begin{bmatrix} \frac{\partial P_1}{\partial S} & \frac{\partial P_1}{\partial H} & \frac{\partial P_1}{\partial I} & \frac{\partial P_1}{\partial Q} \\ \frac{\partial P_2}{\partial S} & \frac{\partial P_2}{\partial H} & \frac{\partial P_2}{\partial I} & \frac{\partial P_2}{\partial Q} \\ \frac{\partial P_3}{\partial S} & \frac{\partial P_3}{\partial H} & \frac{\partial P_3}{\partial I} & \frac{\partial P_3}{\partial Q} \\ \frac{\partial P_4}{\partial S} & \frac{\partial P_4}{\partial H} & \frac{\partial P_4}{\partial I} & \frac{\partial P_4}{\partial Q} \end{bmatrix}. \quad (5)$$

In the following, we determine all the derivatives involved in (5).

$$\begin{aligned} \frac{\partial P_1}{\partial S} &= \frac{1}{1+\varphi(\gamma_1 I+(\omega+\mu))} \frac{\partial P_1}{\partial H} = 0, \quad \frac{\partial P_1}{\partial I} = \frac{\varphi\gamma_1(S+\varphi\Lambda)}{(1+\varphi(\gamma_1 I+(\omega+\mu)))^2}, \quad \frac{\partial P_1}{\partial Q} = 0, \quad \frac{\partial P_2}{\partial S} = 0, \quad \frac{\partial P_2}{\partial H} = \frac{1}{1+\varphi(\tau I+(\omega+\mu))}, \\ \frac{\partial P_2}{\partial I} &= \frac{\varphi\Psi(1+\varphi(\tau I+(\omega+\mu))-\varphi\tau(H+\Psi I+\varphi\epsilon))}{(1+\varphi(\tau I+(\omega+\mu)))^2}, \quad \frac{\partial P_2}{\partial Q} = 0, \quad \frac{\partial P_3}{\partial S} = \frac{-\varphi\gamma_1(I+h\sigma Q)}{(1+\varphi((\omega+\mu+\eta+\Psi)-\gamma_1 S-\tau H))^2}, \quad \frac{\partial P_3}{\partial H} = 0, \quad \frac{\partial P_3}{\partial I} = \\ &= \frac{1}{(1+\varphi((\omega+\mu+\eta+\Psi)-\gamma_1 S-\tau H))}, \quad \frac{\partial P_3}{\partial Q} = \frac{\varphi\sigma}{(1+\varphi((\omega+\mu+\eta+\Psi)-\gamma_1 S-\tau H))}, \quad \frac{\partial P_4}{\partial S} = 0, \quad \frac{\partial P_4}{\partial H} = 0, \quad \frac{\partial P_4}{\partial I} = \frac{\varphi\eta}{1+\varphi(\omega+\mu+\sigma)}, \\ \frac{\partial P_4}{\partial Q} &= \frac{1}{1+\varphi(\omega+\mu+\sigma)}. \end{aligned}$$

By putting all above derivatives in (5), we get

$$J = \begin{bmatrix} \frac{1}{1+\varphi(\gamma_1 I+(\omega+\mu))} & 0 & \frac{\varphi\gamma_1(S+\varphi\Lambda)}{(1+\varphi(\gamma_1 I+(\omega+\mu)))^2} & 0 \\ 0 & \frac{1}{1+\varphi(\tau I+(\omega+\mu))} & \frac{\varphi\Psi(1+\varphi(\tau I+(\omega+\mu))-\varphi\tau(H+\Psi I+\varphi\epsilon))}{(1+\varphi(\tau I+(\omega+\mu)))^2} & 0 \\ \frac{-\varphi\gamma_1(I+h\sigma Q)}{(1+\varphi((\omega+\mu+\eta+\Psi)-\gamma_1 S-\tau H))^2} & 0 & \frac{1}{(1+\varphi((\omega+\mu+\eta+\Psi)-\gamma_1 S-\tau H))} & \frac{\varphi\sigma}{(1+\varphi((\omega+\mu+\eta+\Psi)-\varphi\gamma_1 S-\varphi\tau H))} \\ 0 & 0 & \frac{\varphi\eta}{1+\varphi(\omega+\mu+\sigma)} & \frac{1}{1+\varphi(\omega+\mu+\sigma)} \end{bmatrix}. \quad (6)$$

After putting DFE point $E^0 = \left(\frac{\Lambda}{\omega+\mu}, \frac{\epsilon}{\omega+\mu}, 0, 0\right)$, equation (6) becomes

$$J(E^0) = \begin{bmatrix} \frac{1}{1+\varphi(\omega+\mu)} & 0 & \frac{\varphi\gamma_1(\frac{\Lambda}{\omega+\mu}+\varphi\Lambda)}{(1+\varphi(\omega+\mu))^2} & 0 \\ 0 & \frac{1}{1+\varphi(\omega+\mu)} & \frac{\varphi(\Psi(1+\varphi(\omega+\mu))-\varphi\tau(\frac{\epsilon}{\omega+\mu}+\varphi\epsilon))}{(1+\varphi(\omega+\mu))^2} & 0 \\ 0 & 0 & \frac{1}{(1+\varphi((\omega+\mu+\eta+\Psi)-\gamma_1\frac{\Lambda}{\omega+\mu}-\tau\frac{\epsilon}{\omega+\mu}))} & \frac{\varphi\sigma}{(1+\varphi((\omega+\mu+\eta+\Psi)-\gamma_1\frac{\Lambda}{\omega+\mu}-\tau\frac{\epsilon}{\omega+\mu}))} \\ 0 & 0 & \frac{\varphi\eta}{1+\varphi(\omega+\mu+\sigma)} & \frac{1}{1+\varphi(\omega+\mu+\sigma)} \end{bmatrix}. \quad (7)$$

To find the eigenvalues, we suppose

$$|J(E^0) - \lambda| = 0,$$

i.e.

$$\begin{vmatrix} \frac{1}{1+\varphi(\omega+\mu)} - \lambda & 0 & \frac{+\varphi\gamma_1(\frac{\Lambda}{\omega+\mu}+\varphi\Lambda)}{(1+\varphi(\omega+\mu))^2} & 0 \\ 0 & \frac{1}{1+\varphi(\omega+\mu)} - \lambda & \frac{\varphi(\Psi(1+\varphi(\omega+\mu))-\varphi\tau(\frac{\epsilon}{\omega+\mu}+\varphi\epsilon))}{(1+\varphi(\omega+\mu))^2} & 0 \\ 0 & 0 & \frac{1}{(1+\varphi((\omega+\mu+\eta+\Psi)-\gamma_1\frac{\Lambda}{\omega+\mu}-\tau\frac{\epsilon}{\omega+\mu}))} - \lambda & \frac{\varphi\sigma}{(1+\varphi((\omega+\mu+\eta+\Psi)-\gamma_1\frac{\Lambda}{\omega+\mu}-\tau\frac{\epsilon}{\omega+\mu}))} \\ 0 & 0 & \frac{\varphi\eta}{1+\varphi(\omega+\mu+\sigma)} & \frac{1}{1+\varphi(\omega+\mu+\sigma)} - \lambda \end{vmatrix} = 0. \quad (8)$$

$$\left(\lambda_1 - \frac{1}{1+\varphi(\omega+\mu)}\right) \left(\lambda_2 - \frac{1}{1+\varphi(\omega+\mu)}\right) \begin{vmatrix} \frac{1}{(1+\varphi((\omega+\mu+\eta+\Psi)-\gamma_1\frac{\Lambda}{\omega+\mu}-\tau\frac{\epsilon}{\omega+\mu}))} - \lambda & \frac{\varphi\sigma}{(1+\varphi((\omega+\mu+\eta+\Psi)-\gamma_1\frac{\Lambda}{\omega+\mu}-\tau\frac{\epsilon}{\omega+\mu}))} \\ \frac{\varphi\eta}{1+\varphi(\omega+\mu+\sigma)} & \frac{1}{1+\varphi(\omega+\mu+\sigma)} - \lambda \end{vmatrix} = 0.$$

The above equation provides repeated roots $\lambda_1 = \frac{1}{1+\varphi(\omega+\mu)} < 1$, $\lambda_2 = \frac{1}{1+\varphi(\omega+\mu)} < 1$. To find other eigenvalues, we take

$$\begin{vmatrix} \frac{1}{(1+\varphi((\omega+\mu+\eta+\Psi)-\gamma_1\frac{\Lambda}{\omega+\mu}-\tau\frac{\epsilon}{\omega+\mu}))} - \lambda & \frac{\varphi\sigma}{(1+\varphi((\omega+\mu+\eta+\Psi)-\gamma_1\frac{\Lambda}{\omega+\mu}-\tau\frac{\epsilon}{\omega+\mu}))} \\ \frac{\varphi\eta}{1+\varphi(\omega+\mu+\sigma)} & \frac{1}{1+\varphi(\omega+\mu+\sigma)} - \lambda \end{vmatrix} = 0,$$

i.e.

$$\lambda^2 - \lambda \left(\frac{1}{(1+\varphi((\omega+\mu+\eta+\Psi)-\gamma_1\frac{\Lambda}{\omega+\mu}-\tau\frac{\epsilon}{\omega+\mu}))} + \frac{1}{1+\varphi(\omega+\mu+\sigma)} \right) + \left(\frac{1}{(1+\varphi((\omega+\mu+\eta+\Psi)-\gamma_1\frac{\Lambda}{\omega+\mu}-\tau\frac{\epsilon}{\omega+\mu}))} \times \frac{1}{1+\varphi(\omega+\mu+\sigma)} \right) = 0. \quad (9)$$

Comparing equation (9) with $\lambda^2 - B\lambda + C = 0$, we get $B = \frac{1}{(1+\varphi((\omega+\mu+\eta+\Psi)-\gamma_1\frac{\Lambda}{\omega+\mu}-\tau\frac{\epsilon}{\omega+\mu}))} + \frac{1}{1+\varphi(\omega+\mu+\sigma)}$ and $C =$

$\frac{1}{(1+\varphi((\omega+\mu+\eta+\Psi)-\gamma_1\frac{\Lambda}{\omega+\mu}-\tau\frac{\epsilon}{\omega+\mu}))} \times \frac{1}{1+\varphi(\omega+\mu+\sigma)}$. If $R_0 < 1$, then

- (i) $1 + B + C > 0$
- (ii) $1 - B + C > 0$
- (iii) $C < 1$.

Consequently, all of the Schur-Cohn criteria requirements stated in Lemma 1 are achieved whenever $R_0 < 1$. Thus, the DFE point E^0 of the discrete NSFD scheme (3) is LAS, given that $R_0 < 1$.

Theorem:2 The EE point E^* of the NSFD scheme (3) is LAS for all $\varphi > 0$ whenever $R_0 > 1$.

Proof According to Theorem 1, the Jacobian matrix is represented as follows

$$J = \begin{bmatrix} \frac{1}{1+\varphi(\gamma_1 I+(\omega+\mu))} & 0 & \frac{\varphi\gamma_1(S+\varphi\Lambda)}{(1+\varphi(\gamma_1 I+(\omega+\mu)))^2} & 0 \\ 0 & \frac{1}{1+\varphi(\tau I+(\omega+\mu))} & \frac{\varphi\Psi(1+\varphi(\tau I+(\omega+\mu))-\varphi\tau(H+\Psi I+\varphi\epsilon))}{(1+\varphi(\tau I+(\omega+\mu)))^2} & 0 \\ \frac{-\varphi\gamma_1(I+h\sigma Q)}{(1+\varphi((\omega+\mu+\eta+\Psi)-\gamma_1 S-\tau H))^2} & 0 & \frac{1}{(1+\varphi((\omega+\mu+\eta+\Psi)-\gamma_1 S-\tau H))} & \frac{\varphi\sigma}{(1+\varphi((\omega+\mu+\eta+\Psi)-\varphi\gamma_1 S-\varphi\tau H))} \\ 0 & 0 & \frac{\varphi\eta}{1+\varphi(\omega+\mu+\sigma)} & \frac{1}{1+\varphi(\omega+\mu+\sigma)} \end{bmatrix}. \quad (10)$$

By putting EE point E^* , we get

$$J(E^*) = \begin{bmatrix} \frac{1}{1+\varphi(\gamma_1 I^*+(\omega+\mu))} & 0 & \frac{\varphi\gamma_1(S^*+\varphi\Lambda)}{(1+\varphi(\gamma_1 I^*+(\omega+\mu)))^2} & 0 \\ 0 & \frac{1}{1+\varphi(\tau I^*+(\omega+\mu))} & \frac{\varphi\Psi(1+\varphi(\tau I^*+(\omega+\mu))-\varphi\tau(H+\Psi I^*+\varphi\epsilon))}{(1+\varphi(\tau I^*+(\omega+\mu)))^2} & 0 \\ \frac{-\varphi\gamma_1(I^*+h\sigma Q^*)}{(1+\varphi((\omega+\mu+\eta+\Psi)-\gamma_1 S^*-\tau H^*))^2} & 0 & \frac{1}{(1+\varphi((\omega+\mu+\eta+\Psi)-\gamma_1 S^*-\tau H^*))} & \frac{\varphi\sigma}{(1+\varphi((\omega+\mu+\eta+\Psi)-\varphi\gamma_1 S^*-\varphi\tau H^*))} \\ 0 & 0 & \frac{\varphi\eta}{1+\varphi(\omega+\mu+\sigma)} & \frac{1}{1+\varphi(\omega+\mu+\sigma)} \end{bmatrix}. \quad (11).$$

To find the eigenvalues of (11), we consider

$$|J(E^*) - \lambda| = 0,$$

i.e.

$$\begin{vmatrix} \frac{1}{1+\varphi(\gamma_1 I^*+(\omega+\mu))} - \lambda & 0 & \frac{\varphi\gamma_1(S^*+\varphi\Lambda)}{(1+\varphi(\gamma_1 I^*+(\omega+\mu)))^2} & 0 \\ 0 & \frac{1}{1+\varphi(\tau I^*+(\omega+\mu))} - \lambda & \frac{\varphi\Psi(1+\varphi(\tau I^*+(\omega+\mu))-\varphi\tau(H+\Psi I^*+\varphi\epsilon))}{(1+\varphi(\tau I^*+(\omega+\mu)))^2} & 0 \\ \frac{-\varphi\gamma_1(I^*+h\sigma Q^*)}{(1+\varphi((\omega+\mu+\eta+\Psi)-\gamma_1 S^*-\tau H^*))^2} & 0 & \frac{1}{(1+\varphi((\omega+\mu+\eta+\Psi)-\gamma_1 S^*-\tau H^*))} - \lambda & \frac{\varphi\sigma}{(1+\varphi((\omega+\mu+\eta+\Psi)-\varphi\gamma_1 S^*-\varphi\tau H^*))} \\ 0 & 0 & \frac{\varphi\eta}{1+\varphi(\omega+\mu+\sigma)} & \frac{1}{1+\varphi(\omega+\mu+\sigma)} - \lambda \end{vmatrix} = 0. \quad (12)$$

From equation (12), we obtain the deterministic equation

$$\left(\frac{1}{1+\varphi(\gamma_1 I^*+(\omega+\mu))} - \lambda\right)(\lambda^3 - \lambda^2 K - \lambda L - M) = 0.$$

The above equation gives one eigenvalue $\lambda_1 = \frac{1}{1+\varphi(\gamma_1 I^*+(\omega+\mu))} < 1$. The other eigenvalues can be calculated from

$$\lambda^3 - \lambda^2 K - \lambda L - M = 0, \quad (13)$$

where,

$$K = \frac{1}{1+\varphi(\gamma_1 I^* + (\omega + \mu))} + \frac{-\varphi\gamma_1(I^* + h\sigma Q^*)}{(1+\varphi((\omega + \mu + \eta + \psi) - \gamma_1 S^* - \tau H^*))^2} + \frac{1}{1+(\omega + \mu + \sigma)},$$

$$L = \left(\frac{\varphi\gamma_1(S^* + \varphi\lambda)}{(1 + \varphi(\gamma_1 I^* + (\omega + \mu)))^2} \right) \left(\frac{-\varphi\gamma_1(I^* + h\sigma Q^*)}{(1 + \varphi((\omega + \mu + \eta + \psi) - \gamma_1 S^* - \tau H^*))^2} \right)$$

$$- \left(\frac{1}{1 + \varphi\gamma_1 I^* + \varphi(\omega + \mu)} \right) \left(\frac{-\varphi\gamma_1(I^* + h\sigma Q^*)}{(1 + \varphi((\omega + \mu + \eta + \psi) - \gamma_1 S^* - \tau H^*))^2} \right)$$

$$- \left(\frac{1}{1 + \varphi\gamma_1 I^* + \varphi(\omega + \mu)} \right) \left(\frac{1}{1 + \varphi(\omega + \mu + \sigma)} \right) - \left(\frac{1}{1 + \varphi(\omega + \mu + \sigma)} \right) \left(\frac{-\varphi\gamma_1(I^* + h\sigma Q^*)}{(1 + \varphi((\omega + \mu + \eta + \psi) - \gamma_1 S^* - \tau H^*))^2} \right),$$

$$M = \left(\frac{-\varphi\gamma_1(I^* + h\sigma Q^*)}{(1 + \varphi((\omega + \mu + \eta + \psi) - \gamma_1 S^* - \tau H^*))^2} \right) \left(\frac{\varphi\gamma_1(S^* + \varphi\lambda)}{(1 + \varphi(\gamma_1 I^* + (\omega + \mu)))^2} \right) \left(\frac{1}{1 + \varphi(\omega + \mu + \sigma)} \right)$$

$$- \left(\frac{1}{1 + \varphi(\omega + \mu + \sigma)} \right) \left(\frac{-\varphi\gamma_1(I^* + h\sigma Q^*)}{(1 + \varphi((\omega + \mu + \eta + \psi) - \gamma_1 S^* - \tau H^*))^2} \right) \left(\frac{1}{1 + \varphi\gamma_1 I^* + \varphi(\omega + \mu)} \right)$$

$$- \left(\frac{\varphi\sigma}{(1 + \varphi((\omega + \mu + \eta + \psi) - \varphi\gamma_1 S^* - \varphi\tau H^*))} \right) \left(\frac{\varphi\eta}{1 + \varphi(\omega + \mu + \sigma)} \right)$$

and

It is clear that $K, L, M > 0$ whenever $R_0 > 1$. Also

$$KL - M = \left(\frac{1}{1+\varphi\gamma_1 I^* + \varphi(\omega + \mu)} + \frac{-\varphi\gamma_1(I^* + h\sigma Q^*)}{(1+\varphi((\omega + \mu + \eta + \psi) - \gamma_1 S^* - \tau H^*))^2} + \frac{1}{1+\varphi(\omega + \mu + \sigma)} \right) \left(\frac{\varphi\gamma_1(S^* + \varphi\lambda)}{(1+\varphi(\gamma_1 I^* + (\omega + \mu)))^2} \right)$$

$$\left(\frac{-\varphi\gamma_1(I^* + h\sigma Q^*)}{(1+\varphi((\omega + \mu + \eta + \psi) - \gamma_1 S^* - \tau H^*))^2} \right) - \left(\frac{1}{1+\varphi\gamma_1 I^* + \varphi(\omega + \mu)} \right) \left(\frac{-\varphi\gamma_1(I^* + h\sigma Q^*)}{(1+\varphi((\omega + \mu + \eta + \psi) - \gamma_1 S^* - \tau H^*))^2} \right) -$$

$$\left(\frac{1}{1+\varphi\gamma_1 I^* + \varphi(\omega + \mu)} \right) \left(\frac{1}{1+\varphi(\omega + \mu + \sigma)} \right) - \left(\frac{1}{1+\varphi(\omega + \mu + \sigma)} \right) \left(\frac{-\varphi\gamma_1(I^* + h\sigma Q^*)}{(1+\varphi((\omega + \mu + \eta + \psi) - \gamma_1 S^* - \tau H^*))^2} \right) -$$

$$\left(\frac{-\varphi\gamma_1(I^* + h\sigma Q^*)}{(1+\varphi((\omega + \mu + \eta + \psi) - \gamma_1 S^* - \tau H^*))^2} \right) \left(\frac{\varphi\gamma_1(S^* + \varphi\lambda)}{(1+\varphi(\gamma_1 I^* + (\omega + \mu)))^2} \right) \left(\frac{1}{1+\varphi(\omega + \mu + \sigma)} \right) - \left(\frac{1}{1+\varphi(\omega + \mu + \sigma)} \right)$$

$$\left(\frac{-\varphi\gamma_1(I^* + h\sigma Q^*)}{(1+\varphi((\omega + \mu + \eta + \psi) - \gamma_1 S^* - \tau H^*))^2} \right) \left(\frac{1}{1+\varphi\gamma_1 I^* + \varphi(\omega + \mu)} \right) - \left(\frac{\varphi\sigma}{(1+\varphi((\omega + \mu + \eta + \psi) - \varphi\gamma_1 S^* - \varphi\tau H^*))} \right)$$

$$\left(\frac{\varphi\eta}{1+\varphi(\omega + \mu + \sigma)} \right) > 0.$$

Hence, by employing Routh-Hurwitz criterion of Khatun *et al.* (2020) & Vaz *et al.* (2022), all the solutions of equation (13) must have negative real parts if and only if $R_0 > 1$. As a result, the EE point E^* of NSFD scheme (3) is locally asymptotically stable.

Positivity: The most significant physical characteristics of sub-population (S, H, I, Q) used in the compartmental epidemic flow chart is positivity. The implicit numerical integration scheme and mathematical induction concept are used to study and ensure this fact.

Theorem:3 Let the state variables $S(t), H(t), I(t)$ and $Q(t)$ involved in the scheme are positive at $t = 0$; furthermore, if Additionally, every parameter is positive, then $S_{n+1} \geq 0, H_{n+1} \geq 0, I_{n+1} \geq 0$ and $Q_{n+1} \geq 0$.

Proof:

Using the mathematical induction principle and taking into consideration equation (3), we proceed on as follows:

$$\left. \begin{aligned} S_{n+1} &= \frac{S_n + \varphi\Lambda}{(1 + \varphi(\gamma_1 I_n + (\omega + \mu)))} \\ H_{n+1} &= \frac{H_n + \varphi(\epsilon + \Psi I_n(t))}{(1 + \varphi(\tau I_n + (\omega + \mu)))} \\ I_{n+1} &= \frac{I_n + \varphi\sigma Q_n(t)}{(1 + \varphi((\omega + \mu + \eta + \Psi) - \gamma_1 S_n - \tau H_n))} \\ Q_{n+1} &= \frac{Q_n + \varphi\eta I_n}{(1 + \varphi(\omega + \mu + \sigma))} \end{aligned} \right\} \quad (14)$$

First, we Substitute $n = 0$ in above equations and reached.

$$S_1 = \frac{S_0 + \varphi\Lambda}{(1 + \varphi(\gamma_1 I_0 + (\omega + \mu)))} \geq 0$$

Similarly,

$$\left. \begin{aligned} H_1 &= \frac{H_0 + \varphi(\epsilon + \Psi I_0(t))}{(1 + \varphi(\tau I_0 + (\omega + \mu)))} \geq 0 \\ I_1 &= \frac{I_0 + \varphi\sigma Q_0(t)}{(1 + \varphi((\omega + \mu + \eta + \Psi) - \gamma_1 S_0 - \tau H_0))} \geq 0 \\ Q_1 &= \frac{Q_0 + \varphi\eta I_0}{(1 + \varphi(\omega + \mu + \sigma))} \geq 0 \end{aligned} \right\}$$

Now, we put $n = 1$ in equations (14).

$$S_2 = \frac{S_1 + \varphi\Lambda}{(1 + \varphi(\gamma_1 I_1 + (\omega + \mu)))} \geq 0$$

Similarly,

$$\left. \begin{aligned} H_2 &= \frac{H_1 + \varphi(\epsilon + \Psi I_1(t))}{(1 + \varphi(\tau I_1 + (\omega + \mu)))} \geq 0 \\ I_2 &= \frac{I_1 + \varphi\sigma Q_1(t)}{(1 + \varphi((\omega + \mu + \eta + \Psi) - \gamma_1 S_1 - \tau H_1))} \geq 0 \\ Q_2 &= \frac{Q_1 + \varphi\eta I_1}{(1 + \varphi(\omega + \mu + \sigma))} \geq 0 \end{aligned} \right\}$$

Moreover, let us assume that the above system (14) ensures the positive property for the values of $n = 2, 3, 4, \dots, n - 1$, i.e., $S_n \geq 0, H_n \geq 0, I_n \geq 0$, and $Q_n \geq 0$ for $n = 2, 3, 4, \dots, n - 1$ and sub-population (S, H, I, Q) .

Now, for $n \in Z$,

$$\left. \begin{aligned} S_{n+1} &= \frac{S_n + \varphi\Lambda}{(1 + \varphi(\gamma_1 I_n + (\omega + \mu)))} \geq 0 \\ H_{n+1} &= \frac{H_n + \varphi(\epsilon + \Psi I_n(t))}{(1 + \varphi(\tau I_n + (\omega + \mu)))} \geq 0 \\ I_{n+1} &= \frac{I_n + \varphi\sigma Q_n(t)}{(1 + \varphi((\omega + \mu + \eta + \Psi) - \gamma_1 S_n - \tau H_n))} \geq 0 \\ Q_{n+1} &= \frac{Q_n + \varphi\eta I_n}{(1 + \varphi(\omega + \mu + \sigma))} \geq 0 \end{aligned} \right\}$$

Thus, proposed approach confirms the positive for the state variables $S(t), H(t), I(t)$ and $Q(t) \forall n \in Z^+$.

Boundedness:

Theorem:4 Suppose S_0, H_0, I_0 and Q_0 are finite such that $S_0 + H_0 + I_0 + Q_0 \leq 1$. Then discretized state variables, $S_{n+1}, H_{n+1}, I_{n+1}$ and Q_{n+1} are bounded by recrossing defined real constant e_{n+1} such that $S_{n+1}, H_{n+1}, I_{n+1}$ and $Q_{n+1} < e_{n+1}$ for all $n \in Z^+$ where $e_{n+1} = 4e_n + h\varphi\Lambda + h\varphi(\epsilon + \Psi I_n) + h\varphi\sigma Q_n + h\varphi\eta I_n$ and $e_{n+1} = 4 + h\varphi[\Lambda + \epsilon + I_0(\Psi + \eta) + \sigma Q_0]$.

Proof: Examining the equations for the sub-population (S, H, I, Q) in the implicit numerical integration method.

$$\begin{aligned} S_{n+1}(1 + \varphi h(\gamma_1 I_n + (\omega + \mu))) &= S_n + h\varphi\Lambda \\ H_{n+1}(1 + \varphi h(\tau I_n + (\omega + \mu))) &= H_n + h\varphi(\epsilon + \Psi I_n) \\ I_{n+1}(1 + \varphi h((\omega + \mu + \eta + \Psi) - \gamma_1 S_n - \tau H_n)) &= I_n + h\varphi\sigma Q_n \\ Q_{n+1}(1 + \varphi h(\omega + \mu + \sigma)) &= Q_n + h\varphi\eta I_n \end{aligned}$$

Sum all the above equations,

$$\begin{aligned} \Rightarrow S_{n+1}(1 + \varphi h(\gamma_1 I_n + (\omega + \mu))) &+ H_{n+1}(1 + \varphi h(\tau I_n + (\omega + \mu))) + I_{n+1}(1 + \varphi h((\omega + \mu + \eta + \Psi) - \gamma_1 S_n - \tau H_n)) \\ &+ Q_{n+1}(1 + \varphi h(\omega + \mu + \sigma)) = S_n + h\varphi\Lambda + H_n + h\varphi(\epsilon + \Psi I_n) + I_n + h\varphi\sigma Q_n + Q_n + h\varphi\eta I_n \\ \Rightarrow (S_{n+1} + H_{n+1} + I_{n+1} + Q_{n+1})(1 + \varphi h(\omega + \mu)) &+ \varphi h[\gamma_1 I_n S_{n+1} + \tau I_n H_n + I_{n+1}(\eta + \Psi - \gamma_1 S_n + \tau H_n + \sigma Q_{n+1})] \\ &= (S_n + H_n + I_n + Q_n) + h\varphi[\Lambda + \epsilon + I_n(\Psi + \eta) + \sigma Q_n] \end{aligned}$$

By substituting $n = 0$, in above equation,

$$\begin{aligned} &\Rightarrow (S_1 + H_1 + I_1 + Q_1)(1 + \phi h(\omega + \mu)) + \phi h[\gamma_1 I_0 S_1 + \tau I_0 H_0 + I_1(\eta + \Psi - \gamma_1 S_0 + \tau H_0 + \sigma Q_1)] = \\ &(S_0 + H_0 + I_0 + Q_0) + h\phi[\Lambda + \epsilon + I_0(\Psi + \eta) + \sigma Q_0] \\ &\Rightarrow (S_1 + H_1 + I_1 + Q_1)(1 + \phi h(\omega + \mu)) + \phi h[\gamma_1 I_0 S_1 + \tau I_0 H_0 + I_1(\eta + \Psi - \gamma_1 S_0 + \tau H_0 + \sigma Q_1)] < 4 + \\ &h\phi[\Lambda + \epsilon + I_0(\Psi + \eta) + \sigma Q_0] = e_1 \\ &\Rightarrow (S_1 + H_1 + I_1 + Q_1)(1 + \phi h(\omega + \mu)) + \phi h[\gamma_1 I_0 S_1 + \tau I_0 H_0 + I_1(\eta + \Psi - \gamma_1 S_0 + \tau H_0 + \sigma Q_1)] \leq e_1 \\ &\Rightarrow S_1(1 + \phi h(\gamma_1 I_0 + (\omega + \mu))) + H_1(1 + \phi h(\tau I_0 + (\omega + \mu))) + I_1(1 + \phi h((\omega + \mu + \eta + \Psi) - \gamma_1 S_0 - \tau H_0)) \\ &\quad + Q_1(1 + \phi h(\omega + \mu + \sigma)) \leq e_1 \\ &\quad S_1 \leq e_1, H_1 \leq e_1, I_1 \leq e_1, Q_1 \leq e_1 \end{aligned}$$

By substituting $n = 1$, in above equation,

$$\begin{aligned} &\Rightarrow (S_2 + H_2 + I_2 + Q_2)(1 + \phi h(\omega + \mu)) + \phi h[\gamma_1 I_1 S_2 + \tau I_1 H_1 + I_1(\eta + \Psi - \gamma_1 S_1 + \tau H_1 + \sigma Q_1)] \\ &\quad = (S_1 + H_1 + I_1 + Q_1) + h\phi[\Lambda + \epsilon + I_1(\Psi + \eta) + \sigma Q_1] \\ &\Rightarrow (S_2 + H_2 + I_2 + Q_2)(1 + \phi h(\omega + \mu)) + \phi h[\gamma_1 I_1 S_2 + \tau I_1 H_1 + I_1(\eta + \Psi - \gamma_1 S_1 + \tau H_1 + \sigma Q_1)] \leq e_1 \\ &\Rightarrow S_2(1 + \phi h(\gamma_1 I_1 + (\omega + \mu))) + H_2(1 + \phi h(\tau I_1 + (\omega + \mu))) + I_2(1 + \phi h((\omega + \mu + \eta + \Psi) - \gamma_1 S_1 - \tau H_1)) \\ &\quad + Q_2(1 + \phi h(\omega + \mu + \sigma)) \leq e_1 \\ &\quad S_2 \leq e_1, H_2 \leq e_1, I_2 \leq e_1, Q_2 \leq e_1 \\ &\Rightarrow S_{n+1}(1 + \phi h(\gamma_1 I_n + (\omega + \mu))) + H_{n+1}(1 + \phi h(\tau I_n + (\omega + \mu))) \\ &\quad + I_{n+1}(1 + \phi h((\omega + \mu + \eta + \Psi) - \gamma_1 S_n - \tau H_n)) + Q_{n+1}(1 + \phi h(\omega + \mu + \sigma)) \\ &\quad < 4e_n + h\phi\Lambda + h\phi(\epsilon + \Psi I_n) + h\phi\sigma Q_n + h\phi\eta I_n = e_{n+1} \\ &\quad S_{n+1} < e_{n+1}, H_{n+1} < e_{n+1}, I_{n+1} < e_{n+1}, Q_{n+1} < e_{n+1} \end{aligned}$$

Hence, $S_{n+1}, H_{n+1}, I_{n+1}$ and Q_{n+1} are bordered by $\mathbb{R} e_{n+1} \forall n \in \mathbb{Z}^+$.

4 Global stability of equilibria

Using the same criterion as provided in Allehiyani et al. (2022), we demonstrate the global asymptotic stability (GAS) of DFE and DEE points for the NSFD scheme (3) in the following subsection.

Theorem:5 The DFE point E^0 of the NSFD scheme (3) is GAS for all $\phi > 0$ whenever $R_0 \leq 1$, as presented in Fig.2 (a-d).

Proof If we choose $\sigma > 0$, $\exists m_0$ for any $m \geq m_0$, $S_{n+1} < \frac{\Lambda}{\omega + \mu} + \sigma$. Consider the sequence $\{M(n)\}$ define by

$$M(n) = \phi \Lambda S_{n+1} I_n + \phi \Lambda I_n - C_2 H_n + \Psi I_n + \frac{\eta}{C_3} Q_n,$$

where $C_2 = (\omega + \mu)$ and $C_3 = (\omega + \mu + \sigma)$. From above, we can write

$$M(n+1) - M(n) = \phi \Lambda S_{n+2} I_n + \Psi I_{n+1} + C_2 H_{n+1} + \frac{\eta}{C_3} Q_{n+1} - \phi \tau S_{n+1} I_n - \Psi I_n - C_2 H_n - \frac{\eta}{C_3} Q_n$$

$$\begin{aligned}
& +\varphi\Delta S_{n+1}I_n \\
& = \varphi\Delta S_{n+2}I_n + \Psi(I_{n+1} - I_n) + C_2(H_{n+1} - H_n) + \frac{\eta}{C_3}(Q_{n+1} - Q_n).
\end{aligned}$$

After simple calculations, we obtain

$$\begin{aligned}
& = \varphi\Delta S_{n+2}I_n + \Delta\Psi(\gamma_1 S_n(t)I_n(t) + \tau H_n(t)I_n(t) + \sigma Q_n - (\omega + \mu + \eta + \\
& \quad \Psi)I_n(t)) + C_2(\alpha - \tau H_n(t)I_n(t) + \Psi I_n - (\omega + \mu)H_n(t)) + \frac{\eta}{C_3}(\eta I_{n+1}(t) - \\
& \quad (\omega + \mu + \delta)Q_n(t)) - \varphi\Delta S_{n+1}I_n. \\
& = \left(\varphi\Delta S_{n+2}I_n + \varphi\Delta\Psi \left(\sigma Q_n - C_1 I_n(t) + \Psi I_n - C_2 H_n(t) + \frac{\eta}{C_3} \varphi(\eta I_{n+1}(t) - C_3 Q_n(t)) \right) \right),
\end{aligned}$$

where $C_1 = (\omega + \mu + \eta + \Psi)$.

$$\begin{aligned}
& = \varphi \left(\Delta S_{n+2}I_n + \Delta\Psi \left(\sigma Q_n - C_1 I_n(t) + \Psi I_n - C_2 H_n(t) + \frac{\eta}{C_3} (\eta I_{n+1}(t) - C_3 Q_n(t)) \right) \right) \\
& \cdot \\
& = \varphi \left(\Delta S_{n+2}I_n + \Delta\Psi \left(\Delta\Psi\sigma Q_n - \Delta\Psi C_1 I_n(t) + \Delta\Psi^2 I_n - \Psi\Delta C_2 H_n(t) + \right. \right. \\
& \quad \left. \left. \frac{\Delta\Psi}{C_3} (I_{n+1}(t) - \eta C_3 Q_n(t)) \right) \right).
\end{aligned}$$

We can choose a positive integer τ such that

$$\begin{aligned}
\tau S_{n+2}I_n & \leq q(H_{n+1} + C_1 I_{n+1} + C_3 Q_{n+1}) \\
& \leq q \left(H_{n+1} \left(\left(1 + C_1 \frac{\Psi}{C_2} + C_2 \frac{\eta}{C_2} \right) - \frac{D}{C_3} \right) \right) \\
& \leq q \left(H_{n+1} \left(1 + \frac{C_2 R_0}{(\gamma_1 \Delta + \tau \epsilon)(\omega + \mu)[(\omega + \mu + \eta + \Psi)(\omega + \mu + \sigma) - \sigma \eta]} - (\eta C_3 (D + 1)) - \frac{D}{C_3} \right) \right).
\end{aligned}$$

If $R_0 \leq 1$, and because η is small enough, we conclude that $M(n+1) - M(n) \leq 0$ and $\lim_{n \rightarrow \infty} I_n = 0$ for any $n \geq 0$.

Therefore, we conclude that $\{M(n)\}_{n=0}^{\infty}$ is a monotonic decreasing sequence and $\lim_{n \rightarrow \infty} S_n = \frac{\Delta}{\omega + \mu}$, $\lim_{n \rightarrow \infty} Q_n = \frac{\epsilon}{\omega + \mu}$. Hence, when $R_0 \leq 1$, the DFE point E^0 is GAS.

Theorem:6 The EE point E^* of the NSFD scheme (3) is GAS for all $\varphi > 0$ whenever $R_0 \geq 1$, as presented in Fig.3 (a-d).

Proof: We develop a sequence $\{W(n)\}$ so that

$$W(n) = \frac{1}{\varphi H^*} g\left(\frac{S_n}{S^*}\right) + \frac{1}{\varphi S^*} g\left(\frac{H_n}{H^*}\right) + \frac{\Psi I^*}{\varphi C_3 S^* I^*} g\left(\frac{I_n}{I^*}\right) + \frac{\tau Q^*}{h \varphi S^* H^*} g\left(\frac{Q_n}{Q^*}\right),$$

where $C_3 = (\omega + \mu + \sigma)$. Suppose that $g(y) = y - 1 - \ln(y)$ for all $y \in R^+$, then $0 \leq g(y)$ and $g(y) = 0$ if $y = 1$.

We have

$$g\left(\frac{S_{n+1}}{S^*}\right) - g\left(\frac{S_n}{S^*}\right) = \frac{S_{n+1} - S_n}{S^*} - \ln\left(\frac{S_{n+1}}{S_n}\right)$$

$$\begin{aligned}
&\leq \frac{(S_{n+1}-S^*)(S_{n+1}-S_n)}{S_{n+1}S^*} \\
&= \frac{(S_{n+1}-S^*)}{S_{n+1}S^*} \varphi(\Lambda - \gamma_1 S_{n+1}(t)I_n(t) - (\omega + \mu)S_{n+1}(t)) \\
&= \frac{(S_{n+1}-S^*)}{S_{n+1}S^*} \varphi(\gamma_1 S_{n+1}(t)I_n(t) + (\omega + \mu)S_{n+1}(t) - \gamma_1 S_{n+1}(t)I_n(t) - (\omega + \mu)S_{n+1}(t)) \\
&= \varphi\left((S_{n+1} - S^*)(-(\omega + \mu)(S_{n+1} - S^*) - \gamma_1 I^*(S_{n+1} - S^*))\right) \\
&= \left(\frac{-(\omega + \mu)(S_{n+1} - S^*)^2}{S_{n+1}S^*} + \varphi\gamma_1 I^* \left(1 - \frac{S^*}{S_{n+1}}\right) \left(\frac{H_n S_{n+1}}{H^* S^*} - 1\right)\right). \\
g\left(\frac{H_{n+1}}{H^*}\right) - g\left(\frac{H_n}{H^*}\right) &= \frac{H_{n+1} - H_n}{H^*} - \ln\left(\frac{H_{n+1}}{H_n}\right) \\
&\leq \frac{(H_{n+1} - H^*)}{H_{n+1}H^*} (\in -\tau H_n(t)I_n(t) + \Psi I_n - (\omega + \mu)H_n(t)) \\
&\leq \frac{(H_{n+1} - H^*)}{H_{n+1}H^*} \left(\tau H_n(t)I_n(t) - \frac{I_{n+1}S^*}{I^*} - \frac{\Psi I_{n+1}A^*}{I^*} + \Psi H_{n+1}(t)\right) \\
&= \left(1 - \frac{I^*}{I_{n+1}}\right) \left(\frac{\Psi \varphi I^*}{H^*} \left(\frac{I_{n+1}}{I^*} - \frac{H_{n+1}}{H^*}\right) + \left(1 - \frac{I^*}{I_{n+1}}\right) \left(\frac{\varphi S^* H^*}{H^*} \left(\frac{S_{n+1}\tau I_n}{S^*} - \frac{I_{n+1}S^*}{C^*}\right)\right)\right),
\end{aligned}$$

Similarly

$$\begin{aligned}
g\left(\frac{I_{n+1}}{I^*}\right) - g\left(\frac{I_n}{I^*}\right) &= \frac{I_{n+1} - I_n}{I^*} - \ln\left(\frac{I_{n+1}}{I_n}\right) \\
&\leq \frac{(I_{n+1} - I^*)(I_{n+1} - I_n)}{I_{n+1}I^*} \\
&\leq \frac{(I_{n+1} - I^*)}{I_{n+1}I^*} (\gamma_1 S_n(t)I_n(t) + \tau H_n(t)I_n(t) + \sigma Q_n - (\omega + \mu + \eta + \Psi)I_n(t)) \\
&\leq \frac{(I_{n+1} - I^*)}{I_{n+1}I^*} (\gamma_1 S_n(t)I_n(t) + \tau H_n(t)I_n(t) + \sigma Q_n - C_4 I_{n+1})
\end{aligned}$$

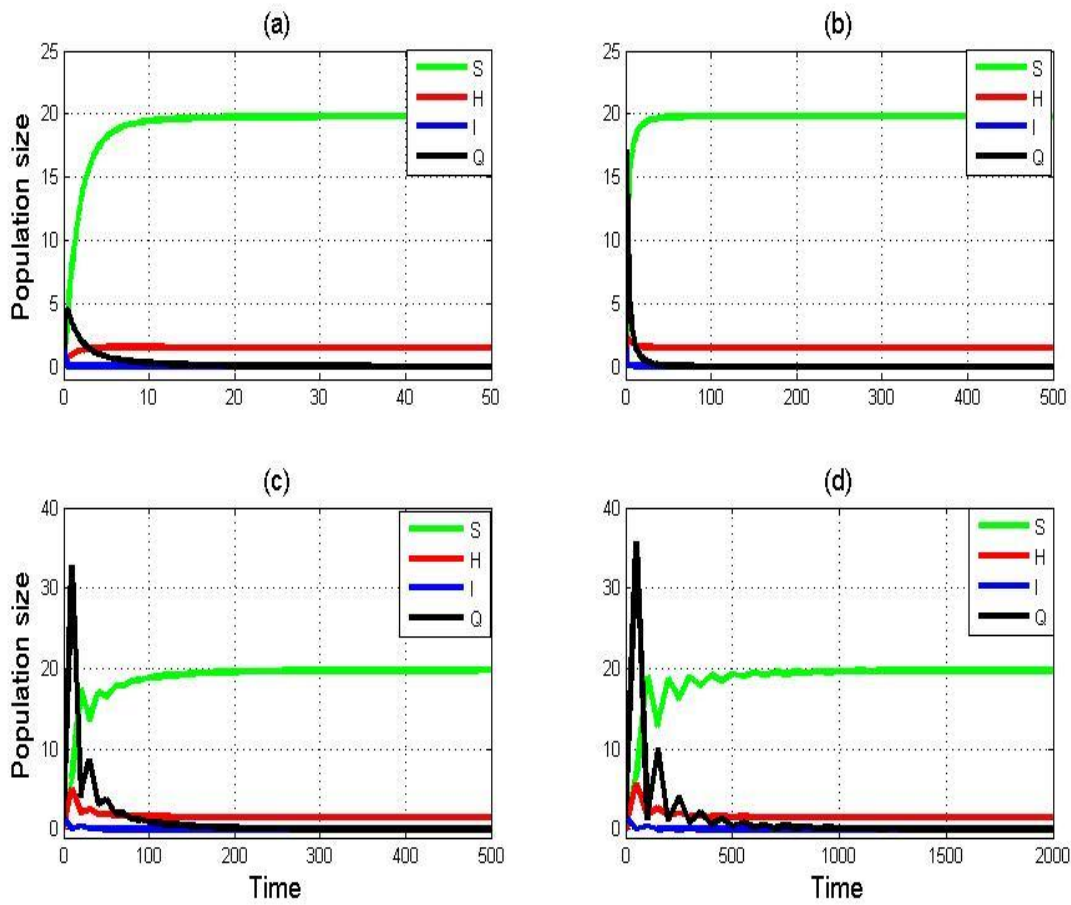


Figure 2

In **Figure 2** the numerical results obtained through most valuable NSFD scheme for DFE points. The numerical simulations show unconditionally convergence as shown in Figure 2 (a), (b), (c) and (d). This simulations results conclude that NSFD scheme always show positive results at all finite step sizes. The DFE point stability by using NSFD scheme with (a) $\varphi = 0.1$, (b) $\varphi = 1$, (c) $\varphi = 10$, and (d) $\varphi = 50$. Other parameter quantities remain fixed as $\Lambda = 12, \gamma_1 = 0.8, \omega = 0.006, \sigma = 0.2, \Psi = 1.9, \tau = 0.02, \epsilon = 0.9, \mu = 0.6$, and $\eta = 19.7$.

where $C_4 = (\omega + \mu + \eta + \Psi)$

$$= C_4 \varphi \left(1 - \frac{I^*}{I_{n+1}} \right) \left(\frac{H_{n+1}}{H^*} - \frac{I_{n+1}}{I^*} \right),$$

and

$$g\left(\frac{Q_{n+1}}{Q^*}\right) - g\left(\frac{Q_n}{Q^*}\right) = \frac{Q_{n+1} - Q_n}{Q^*} - \ln\left(\frac{Q_{n+1}}{Q_n}\right) \leq \frac{(Q_{n+1} - Q^*)(Q_{n+1} - Q_n)}{Q_{n+1}Q^*}$$

$$\begin{aligned} &\leq \frac{(Q_{n+1} - Q^*)}{Q_{n+1}Q^*} (\eta I_{n+1}(t) - (\omega + \mu + \sigma)Q_n(t)) \\ &\leq \left(1 - \frac{Q^*}{Q_{n+1}}\right) \left(\eta \frac{I_{n+1}}{Q^*} - c_5 \frac{Q_{n+1}}{Q^*}\right), \end{aligned}$$

where $c_5 = (\omega + \mu + \sigma)$.

The difference of $W(n)$ satisfies

$$\begin{aligned} W(n+1) - W(n) &= \frac{1}{hA^*} \left(g\left(\frac{S_{n+1}}{S^*}\right) - g\left(\frac{S_n}{S^*}\right) + \frac{1}{\varphi S^*} g\left(\frac{H_{n+1}}{H^*}\right) - g\left(\frac{H_n}{H^*}\right) \right) + \frac{\psi I^*}{\varphi C_3 S^* H^*} \left(g\left(\frac{I_{n+1}}{I^*}\right) - \right. \\ &\quad \left. g\left(\frac{I_n}{I^*}\right) \right) + \frac{\tau Q^*}{\varphi C_2 S^* H^*} \left(g\left(\frac{Q_{n+1}}{Q^*}\right) - g\left(\frac{Q_n}{Q^*}\right) \right) \\ &\leq \left(\left(\frac{-(\omega + \mu)(S_{n+1} - S^*)^2}{S_{n+1} S^*} + \varphi \gamma_1 I^* \left(1 - \frac{S^*}{S_{n+1}}\right) \left(\frac{H_n}{H^*} \frac{S_{n+1}}{S^*} - 1\right) \right) \right) - \left(1 - \frac{I^*}{I_{n+1}}\right) \\ &\quad \left(\frac{\psi \varphi I^*}{H^*} \left(\frac{I_{n+1}}{I^*} - \frac{H_{n+1}}{H^*}\right) + \left(\left(1 - \frac{I^*}{I_{n+1}}\right) \left(\frac{\varphi S^* H^*}{H^*} \left(\frac{\tau I_n S_{n+1}}{S^*} - \frac{I_{n+1} S^*}{C^*}\right) \right) \right) \right) - \frac{\psi I^*}{\varphi C_3 S^* H^*} \\ &\quad \left(C_4 \varphi \left(1 - \frac{I^*}{I_{n+1}}\right) \left(\frac{H_{n+1}}{H^*} - \frac{I_{n+1}}{I^*}\right) - \frac{\tau Q^*}{\varphi C_2 S^* H^*} \left(\varphi \left(1 - \frac{Q^*}{Q_{n+1}}\right) \left(\frac{H_{n+1}}{H^*} - \frac{Q_{n+1}}{Q^*}\right) \right) \right) \\ &\leq \frac{-\tau \varphi (S_{n+1} - S^*)^2}{S_{n+1} S^*} - \frac{\psi \varphi H^*}{I^*} \left(\frac{I^*}{I_{n+1}} \frac{H_n}{H^*} \frac{S_{n+1}}{S^*} - 2 - \frac{H_n}{H^*} + \frac{S^*}{S_{n+1}} + \frac{H_{n+1}}{H^*}\right) \\ &\quad - \frac{1}{\varphi S^*} \left(\frac{I^* H_{n+1}}{I_{n+1} I^*} + \frac{H^* I_{n+1}}{H_{n+1} I^*} - 2\right) - \frac{\tau Q^*}{\varphi C_2 S^* H^*} \left(\frac{I^* Q_{n+1}}{I_{n+1} Q^*} + \frac{Q^* I_{n+1}}{Q_{n+1} I^*} - 2\right) \\ &\leq \frac{-\tau \varphi (S_{n+1} - S^*)^2}{S_{n+1} S^*} - \frac{1}{\varphi H^*} \left(g\left(\frac{S^*}{S_{n+1}}\right) + g\left(\frac{H_{n+1}}{H^*}\right) \right) + g\left(\frac{I^*}{I_{n+1}} \frac{H_n}{H^*} \frac{S_{n+1}}{S^*}\right) - \\ &\quad g\left(\frac{H_n}{H^*}\right) - \frac{1}{\varphi S^*} \left(g\left(\frac{H^* I_{n+1}}{H_{n+1} I^*}\right) + g\left(\frac{I^* H_{n+1}}{I_{n+1} I^*}\right) \right) - \frac{\tau Q^*}{\varphi C_2 S^* H^*} \left(g\left(\frac{H^* Q_{n+1}}{H_{n+1} Q^*}\right) + g\left(\frac{Q^* H_{n+1}}{Q_{n+1} H^*}\right) \right). \end{aligned}$$

Hence, $\{W(n)\}$ is decreasing sequence for any $n \geq 0$ which is monotonic. As $\{W(n)\} \geq 0$ and $\lim_{n \rightarrow \infty} (W(n+1) - W(n)) = 0$, consequently we achieve $\lim_{n \rightarrow \infty} S_{n+1} = S^*$, $\lim_{n \rightarrow \infty} H_{n+1} = H^*$, $\lim_{n \rightarrow \infty} I_{n+1} = I^*$ and $\lim_{n \rightarrow \infty} Q_{n+1} = Q^*$. Hence, if $R_0 \geq 1$, the EE point E^* is GAS.

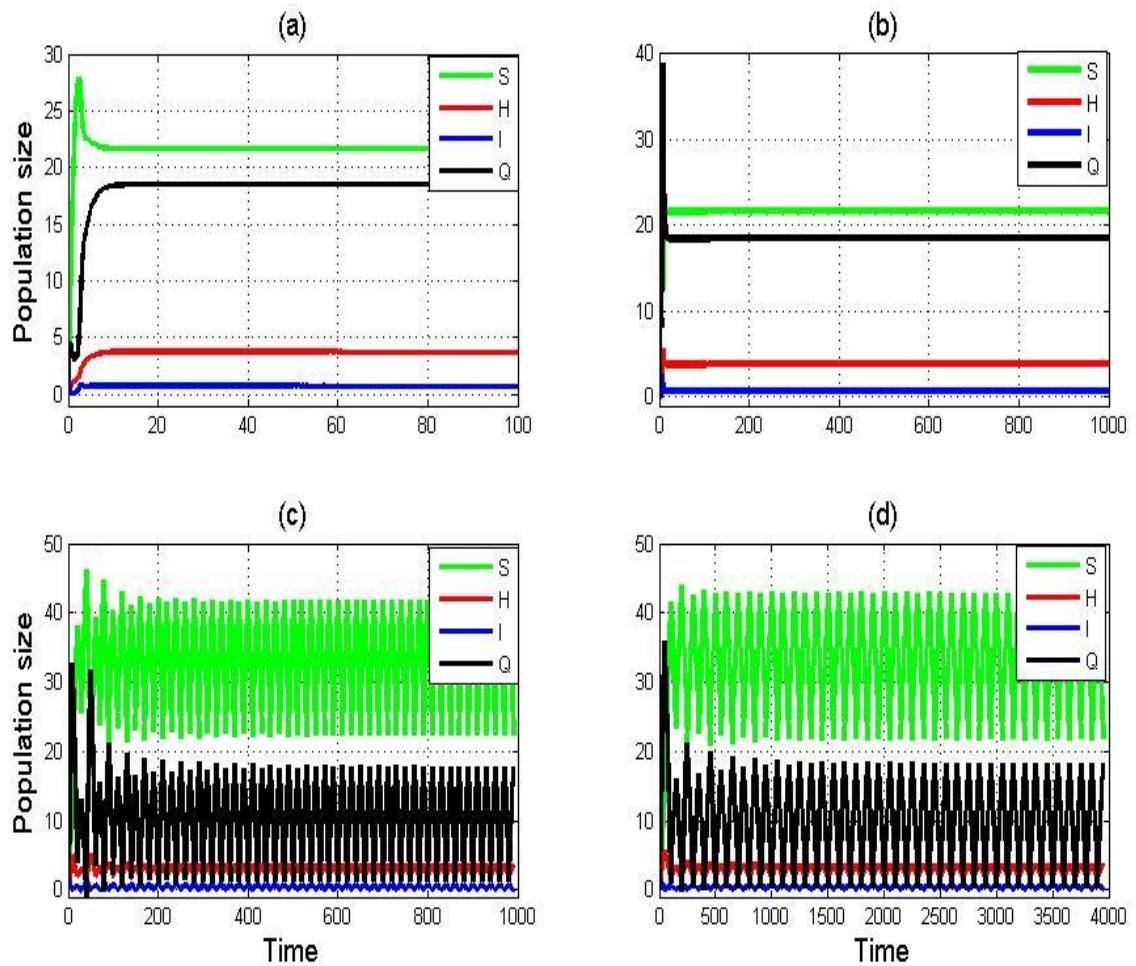


Figure 3. Numerical simulations for system (1)

In **Figure 3** numerical simulations for system (1) shows the convergence results for endemic points through NSFD schemes. The graph (a), (b), (c) and (d) show the positive results for different step size which shows that the NSFD scheme is unconditionally convergent for endemic points. The EE point stability by using NSFD scheme with (a) $\varphi=0.1$, (b) $\varphi=1$, (c) $\varphi=10$, and (d) $\varphi = 50$. Other parameter quantities remain fixed as $\Lambda =26.2$, $\gamma_1 = 0.8$, $\omega = 0.006$, $\sigma = 0.2$, $\Psi = 1.9$, $\tau = 0.02$, $\epsilon = 0.9$ $\mu = 0.6$, and $\eta = 19.7$.

5. Conclusions

To better understand the dynamics of COVID-19 disease transmission, a novel mathematical model of COVID-19 is considered and analyzed in the present paper. The important threshold quantity R_0 is structured for the model which is crucial in the investigation of DFE and EE points stability. The discrete NSFD scheme is designed to

explore the complicated dynamical behaviour of nonlinear continuous model. The aforementioned technique yields more accurate results that are both mathematically and biologically plausible and is unconditionally convergent. For NSFD scheme, the local and global stability of both equilibria are illustrated using a variety of criteria and conditions. The discrete NSFD technique has been shown to be a robust, effective, and vigorously accurate method that provides a clear representation of continuous model for all time step sizes. In order to demonstrate the validity of the theoretical and mathematical work, numerical simulations are also produced.

Acknowledgements

We gratefully acknowledge the financial support provided by Universiti Sains Malaysia (Main Campus) and the Malaysian International Scholarship.

Author Contribution Statement

Shah Zeb: Conceptualization, Methodology, Software, Supervision, Writing original draft. **Noreen Kausar:** Data collection, Writing original draft. **Muhammad Rafiq:** Supervision, Writing, Reviewing and Editing. **Muhammad Irfan:** Visualization, Investigation. **Ihsan Ullah Khan:** Visualization, Investigation. **Muhammad Bilal:** Software, Validation.

Data Availability

The data used to support the findings of this study are included within the article.

Declaration of Generative AI and AI-Assisted Technologies

The authors declare they have not used Artificial Intelligence (AI) tools were used in the creation of this article. Chat-Gpt and Quilt-bolt are used for rephrasing.

Conflicts of Interest

The authors declare that they have no conflicts of interest.

REFERENCES

- Aba Oud, M. A., Ali, A., Alrabaiah, H., Ullah, S., Khan, M. A., & Islam, S. (2021). A fractional order mathematical model for COVID-19 dynamics with quarantine, isolation, and environmental viral load. *Advances in Difference Equations*, 2021(1), 1–19.
- Adak, D., Majumder, A., & Bairagi, N. (2021). Mathematical perspective of COVID-19 pandemic: Disease extinction criteria in deterministic and stochastic models. *Chaos, Solitons & Fractals*, 142, 110381.
- Ahmad, S. I., Modu, G. U., Yusuf, A., Kumam, P., & Yusuf, I. (2021). A mathematical model of Coronavirus Disease (COVID-19) containing asymptomatic and symptomatic classes. *Results in Physics*, 21, 103776.

Ahmad, S., Owyed, S., Abdel-Aty, A. H., Mahmoud, E. E., Shah, K., & Alrabaiah, H. (2021). Mathematical analysis of COVID-19 via new mathematical model. *Chaos, Solitons & Fractals*, *143*, 110585.

Akinpelu, F. O., & Akinwande, R. (2018). Mathematical model for Lassa fever and sensitivity analysis. *Journal of Scientific and Engineering Research*, *5*(6), 1–9.

Aljohani, A., Shokri, A., & Mukalazi, H. (2024). Analyzing the dynamic patterns of COVID-19 through nonstandard finite difference scheme. *Scientific Reports*, *14*(1), 8466.

Ali, Z., Rabiei, F., Shah, K., & Khodadadi, T. (2021). Qualitative analysis of fractal-fractional order COVID-19 mathematical model with case study of Wuhan. *Alexandria Engineering Journal*, *60*(1), 477–489.

Allehiany, F. M., Dayan, F., Al-Harbi, F. F., Althobaiti, N., Ahmed, N., Rafiq, M., ... Elamin, M. (2022). Bio-inspired numerical analysis of COVID-19 with fuzzy parameters. *Computers, Materials & Continua*, *72*(2), 3213–3229. <https://doi.org/10.32604/cmc.2022.025811>

Acuna-Zegarra, M. A., Diaz-Infante, S., Baca-Carrasco, D., & Olmos-Liceaga, D. (2020). COVID-19 optimal vaccination policies: A modeling study on efficacy, natural and vaccine-induced immunity responses. *medRxiv*. <https://doi.org/10.1101/2020.05.28.20115933> (if known, otherwise leave as medRxiv)

Brauer, F. (2017). Mathematical epidemiology: Past, present, and future. *Infectious Disease Modelling*, *2*(2), 113–127.

Brauer, F., & Chávez, C. C. (2001). *Mathematical models in population biology and epidemiology*. Springer.

Castillo-Chavez, C., Blower, S., Van den Driessche, P., Kirschner, D., & Yakubu, A. A. (Eds.). (2002). *Mathematical approaches for emerging and reemerging infectious diseases: Models, methods, and theory* (Vol. 126). Springer.

Contreras, S., & Priesemann, V. (2021). Risking further COVID-19 waves despite vaccination. *The Lancet Infectious Diseases*, *21*(6), 745–746.

Dang, Q. A., & Hoang, M. T. (2019). Complete global stability of a metapopulation model and its dynamically consistent discrete models. *Qualitative Theory of Dynamical Systems*, *18*(2), 461–475.

Darti, I., & Suryanto, A. (2020). Dynamics of a SIR epidemic model of childhood diseases with a saturated incidence rate: Continuous model and its nonstandard finite difference discretization. *Mathematics*, *8*(9), 1459.

Diekmann, O., Heesterbeek, J. A. P., & Roberts, M. G. (2010). The construction of next-generation matrices for compartmental epidemic models. *Journal of the Royal Society Interface*, 7(47), 873–885. <https://doi.org/10.1098/rsif.2009.0386>

Duan, K., Liu, B., Li, C., Zhang, H., Yu, T., Qu, J., ... Yang, X. (2020). The feasibility of convalescent plasma therapy in severe COVID-19 patients: A pilot study. *medRxiv*.

Elaydi, S. (2005). *An introduction to difference equations* (3rd ed.). Springer.

Francis, A. I., Ghany, S., Gilkes, T., & Umakanthan, S. (2022). Review of COVID-19 vaccine subtypes, efficacy and geographical distributions. *Postgraduate Medical Journal*, 98(1159), 389–394.

Ivorra, B., Ferrández, M. R., Vela-Pérez, M., & Ramos, A. M. (2020). Mathematical modeling of the spread of the coronavirus disease 2019 considering undetected infections: The case of China. *Communications in Nonlinear Science and Numerical Simulation*, 88, 105303.

Jia, J., & Li, P. (2011). Global analysis of an SVEIR epidemic model with partial immunity. *Math Terna*, 8(8), 547–561.

Kaur, S. P., & Gupta, V. (2020). COVID-19 vaccine: A comprehensive status report. *Virus Research*, 288, 198114.

Khan, I. U., Hussain, A., Li, S., & Shokri, A. (2023). Modeling the transmission dynamics of coronavirus using nonstandard finite difference scheme. *Fractal and Fractional*, 7(6), 451.

Khatun, Z., Islam, M. S., & Ghosh, U. (2020). Mathematical modeling of hepatitis B virus infection incorporating immune responses. *Sensors International*, 1, 100017.

Klompas, M., Pandolfi, M. C., Nisar, A. B., Baker, M. A., & Rhee, C. (2022). Association of Omicron vs wild-type SARS-CoV-2 variants with hospital-onset infections in a U.S. regional hospital system. *JAMA*, 328(3), 296–298.

Kumar, D., Singh, J., Al-Qurashi, M., & Baleanu, D. (2019). A new fractional SIRS-SI malaria disease model with vaccines, antimalarial drugs, and spraying. *Advances in Difference Equations*, 2019(1), 1–19.

Mahmoudi, M. R., Heydari, M. H., Qasem, S. N., Mosavi, A., & Band, S. S. (2021). Principal component analysis to study the relations between the spread rates of COVID-19 in high-risk countries. *Alexandria Engineering Journal*, 60(1), 457–464.

Medvedeva, M. A., & Simos, T. E. (2024). An exceedingly effective and inexpensive two-step, fourteenth-order phase-fitting method for solving quantum chemical issues. *Journal of Mathematical Chemistry*, 62(3), 761–801.

Medvedeva, M. A., & Simos, T. E. (2024). A very efficient and sophisticated fourteenth-order phase-fitting method for addressing chemical issues. *Journal of Mathematical Chemistry*, 62(9), 2129–2159.

Mickens, R. E. (1994). *Nonstandard finite difference models of differential equations*. World Scientific.

Moore, S., Hill, E. M., Tildesley, M. J., Dyson, L., & Keeling, M. J. (2021). Vaccination and non-pharmaceutical interventions for COVID-19: A mathematical modelling study. *The Lancet Infectious Diseases*, 21(6), 793–802.

Ogana, W., Juma, V. O., & Bulimo, W. D. (2021). A SIRD model applied to COVID-19 dynamics and intervention strategies during the first wave in Kenya. *medRxiv*.

Ochoche, J. M., & Gweryina, R. I. (2014). A mathematical model of measles with vaccination and two phases of infectiousness. *IOSR Journal of Mathematics*, 10(1), 95–105.

Rao, F., Mandal, P. S., & Kang, Y. (2019). Complicated endemics of an SIRS model with a generalized incidence under preventive vaccination and treatment controls. *Applied Mathematical Modelling*, 67, 38–61.

Rao, P. R. S., Ratnam, K. V., & Murthy, M. S. R. (2018). Stability preserving non-standard finite difference schemes for certain biological models. *International Journal of Dynamics and Control*, 6(4), 1496–1504.

Sardar, T., Nadim, S. S., Rana, S., & Chattopadhyay, J. (2020). Assessment of lockdown effect in some states and overall India: A predictive mathematical study on COVID-19 outbreak. *Chaos, Solitons & Fractals*, 139, 110078.

Shabbir, M. S., Din, Q., Safeer, M., Khan, M. A., & Ahmad, K. (2019). A dynamically consistent nonstandard finite difference scheme for a predator–prey model. *Advances in Difference Equations*, 2019(1), 1–17.

Shokri, A., Khalsaraei, M. M., & Molayi, M. (2022). Nonstandard dynamically consistent numerical methods for an MSEIR model. *Journal of Applied and Computational Mechanics*, 8(1), 196–205.

Simos, T. E. (2024). Efficient multistep algorithms for first-order IVPs with oscillating solutions: II Implicit and predictor–corrector algorithms. *Symmetry*, 16(5), 508.

Vaz, S., & Torres, D. F. M. (2021). A dynamically-consistent nonstandard finite difference scheme for the SICA model. *Mathematical Biosciences and Engineering*, 18(4), 4552–4571.

Zeb, S., Mohd Yatim, S. A., Kamran, A., Kausar, R. and Rafiq, M. (2026). A new delayed SEIR-SEI model for dengue transmission control with sensitivity and competitive mathematical analysis. *Computational Methods for Differential Equations*, 14(1), 470-501.

Zeb, S., Bilal, M., Rafiq, M., Mohd Yatim, S. A., Ali, Z., & Kamran, A. (2024). Structure preserving numerical analysis of HIV/AIDS epidemic model. *International Journal of Mathematical Modelling and Numerical Optimisation*, 15(4), 293–323.

